KJA
Korean Journal of Anesthesiology

Clinical Research Article

Korean J Anesthesiol 2023;76(2):116-127
https://doi.org/10.4097/kja.22324
pISSN 2005-6419 • eISSN 2005-7563

Received: May 31, 2022
Revised: September 19, 2022 (1st); October 14, 2022 (2nd); October 17, 2022 (3rd)
Accepted: October 20, 2022

Corresponding author:
Jonghae Kim, M.D.
Department of Anesthesiology and Pain Medicine, Daegu Catholic University Medical Center, Daegu Catholic University School of Medicine, 33 Duryugongwon-ro 17-gil, Nam-gu, Daegu 42472, Korea
Tel: +82-53-650-4979
Fax: +82-53-650-4517
Email: usmed@cu.ac.kr; usmed12@gmail.com
ORCID: https://orcid.org/0000-0003-1222-0054

*Eugene Kim and Jung A Lim contributed equally to this work as co-first authors.

Previous presentation in conferences:
This work was presented in abstract form at the 33rd International Symposium on the Autonomic Nervous System, Lahaina, Maui, Hawaii, November 2-5, 2022.

Assessment of the changes in cardiac sympathetic nervous activity using the pupil size changes measured in seated patients whose stellate ganglion is blocked by interscalene brachial plexus block

Eugene Kim[1,*], Jung A Lim[2,*], Chang Hyuk Choi[3], So Young Lee[2], Seongmi Kwak[2], Jonghae Kim[2]

[1]Department of Anesthesiology and Pain Medicine, Hanyang University Medical Center, Hanyang University College of Medicine, Seoul, Departments of [2]Anesthesiology and Pain Medicine, [3]Orthopedic Surgery, Daegu Catholic University Medical Center, Daegu Catholic University School of Medicine, Daegu, Korea

Background: As a side effect of interscalene brachial plexus block (ISBPB), stellate ganglion block (SGB) causes reductions in pupil size (Horner's syndrome) and cardiac sympathetic nervous activity (CSNA). Reduced CSNA is associated with hemodynamic instability when patients are seated. Therefore, instantaneous measurements of CSNA are important in seated patients presenting with Horner's syndrome. However, there are no effective tools to measure real-time CSNA intraoperatively. To evaluate the usefulness of pupillometry in measuring CSNA, we investigated the relationship between pupil size and CSNA.

Methods: Forty-two patients undergoing right arthroscopic shoulder surgery under ISBPB were analyzed. Pupil diameters were measured at 30 Hz for 2 s using a portable pupillometer. Bilateral pupil diameters and CSNA (natural-log-transformed low-frequency power [0.04–0.15 Hz] of heart rate variability [lnLF]) were measured before ISBPB (pre-ISBPB) and 15 min after transition to the sitting position following ISBPB (post-sitting). Changes in the pupil diameter ([right pupil diameter for post-sitting – left pupil diameter for post-sitting] – [right pupil diameter for pre-ISBPB – left pupil diameter for pre-ISBPB]) and CSNA (lnLF for post-sitting – lnLF for pre-ISBPB) were calculated.

Results: Forty-one patients (97.6%) developed Horner's syndrome. Right pupil diameter and lnLF significantly decreased upon transition to sitting after ISBPB. In the linear regression model (R^2 = 0.242, P = 0.001), a one-unit decrease (1 mm) in the extent of changes in the pupil diameter reduced the extent of changes in lnLF by 0.659 ln(ms^2/Hz) (95% CI [0.090, 1.228]).

Conclusions: Pupillometry is a useful tool to measure changes in CSNA after the transition to sitting following ISBPB.

Keywords: Arthroscopy; Brachial plexus block; Heart rate; Linear models; Pupil; Shoulder; Sitting position; Stellate ganglion; Sympathetic nervous system.

Introduction

Interscalene brachial plexus block (ISBPB) has been widely used for surgical anesthesia in patients undergoing arthroscopic shoulder surgery [1,2]. However, ISBPB is not with-

out side effects. Local anesthetic placed into the interscalene groove spills out of the groove and spreads along the prevertebral fascia toward the ipsilateral stellate ganglion [3]. Local anesthetic-induced stellate ganglion block (SGB) inhibits the oculosympathetic pathway, resulting in miosis of the ipsilateral pupil (Horner's syndrome). Given that the stellate ganglion synapses with cardiac sympathetic postganglionic fibers [4], SGB also reduces cardiac sympathetic nervous activity (CSNA). Therefore, SGB has been used as one of the methods for cardiac sympathetic denervation to treat medically refractory arrhythmias driven by enhanced CSNA, such as refractory ventricular arrhythmia, long QT syndrome, and inappropriate sinus tachycardia [5–7]. Usually, arthroscopic shoulder surgery is performed with patients seated because the sitting position provides excellent intra-articular visualization, reduces intraoperative blood loss, decreases the incidence of traction neuropathy, and facilitates the conversion to an open procedure [8]. However, after a right SGB, the CSNA does not increase with positional changes from supine to sitting [9] or during head-up tilt [10], unlike normal physiologic conditions where a transition to sitting enhances sympathetic nervous activity (SNA) [9] to compensate for a reduction in the venous return to the heart [11]. Occasionally, a right SGB leads to cardiac arrest during a head-up tilt test [12]. Therefore, the measurement of CSNA is important after the transition to the sitting position when patients present with Horner's syndrome after ISBPB. However, measurement of CSNA using conventional methods is impractical in intraoperative settings [13]. Alternatively, heart rate variability (HRV) is feasible to measure the autonomic nervous activity confined to the heart. Despite the unreliability of the low-frequency power (LF) of HRV, which is reported to represent cardiac autonomic outflow by baroreflexes rather than CSNA [14] and is significantly affected by heart rate [15], LF performs well to reflect changes in CSNA in response to a postural change maneuver or head-up tilt test, which consistently increases SNA [16,17]. Hence, LF is assumed to reliably represent CSNA in seated patients receiving arthroscopic shoulder surgery under ISBPB, similar to subjects undergoing a postural change maneuver or head-up tilt test, because they share the same physiological conditions (reduced venous return to the heart). However, the accurate calculation of LF requires a 4-minute-long electrocardiogram (ECG) waveform [18], so it cannot provide instantaneous information about CSNA. In addition, an ECG waveform is prone to artifacts from movement or electrocauterization, which require manual processing to remove, thereby preventing the automatic calculation of HRV parameters.

Pupil size is controlled by the interplay of the iris sphincter and dilator muscles, which are innervated by the parasympathetic and sympathetic nervous systems, respectively. Therefore, pupillometry is useful to evaluate autonomic nervous activity. Recently, owing to its easy applicability and low cost, pupillometry has been proposed as an alternative method for the assessment of cardiac autonomic nervous activity [19,20] after a significant correlation was found between pupil size and LF at rest in healthy subjects [21,22], during exercise in athletes [20], and during exercise in patients undergoing hemodialysis [19]. In particular, the measurement of pupil size would be useful to assess CSNA in patients receiving SGB to treat atrial fibrillation that prevents the analysis of HRV [23].

However, the relationship between the changes in pupil size and CSNA has not been investigated after transitioning to the sitting position under the influence of ISBPB-induced SGB. Therefore, the usefulness of pupillometry remains unclear for seated patients with ISBPB-induced SGB. In this study, we measured the pupil size and autonomic nervous activity (HRV parameters) of patients in the seated position after ISBPB to test the hypothesis that changes in pupil size are correlated with changes in CSNA before ISBPB and after the transition to sitting following ISBPB.

Materials and Methods

The protocol of this observational study was approved by the Institutional Review Board of Daegu Catholic University Medical Center (IRB no. CR-18-052). Written informed consent was obtained from all patients during their preoperative visits to the outpatient department. The study followed the Good Clinical Practice guidelines and the principles of the Declaration of Helsinki (2013).

We enrolled patients aged 20–60 years with an American Society of Anesthesiologists physical status of 1 who were scheduled to undergo right arthroscopic shoulder surgery under ISBPB. The exclusion criteria were coagulopathy, infection at the ISBPB site, peripheral neuropathy or neurologic sequelae on the operative limb, allergy to local anesthetics or history of allergic shock, contralateral vocal cord palsy, contralateral hemidiaphragmatic paresis or paralysis, contralateral pneumothorax or hemothorax, physiologic anisocoria (a difference in the pupil diameter between both eyes of more than 0.5 mm), severe ptosis precluding measurement of the pupil diameter, arrhythmias, conduction abnormalities on ECG, use of medications that affect cardiac conduction, ischemic heart disease, hypertension, diabetes mellitus, thyroid dysfunction, electrolyte imbalance, psychiatric diseases, and difficulty communicating with the medical personnel.

The patients abstained from alcohol and caffeine-containing products for at least 24 h before surgery. No premedication was

administered to the patients. On arrival to the operating room, the patients were placed in a supine position on the operating table. A pulse oximeter sensor (TruSignal™ SpO_2 Finger Sensor, TS-F-D, GE Healthcare Finland Oy, Finland) and a noninvasive blood pressure cuff were placed over the right index finger and on the left arm, respectively. Three ECG electrodes were placed on both the infraclavicular fossae and left anterior axillary line midway between the costal margin and the iliac crest. Once the ECG and photoplethysmographic (PPG) waveforms were displayed without artifacts on a patient monitor (CARESCPE™ Monitor B650, GE Healthcare Finland Oy, Finland), all the lights in the operating room were turned off, the patient monitor was turned away from the patient, and acclimation commenced under quiet conditions at ambient temperature to stabilize the patients' hemodynamics and autonomic nervous activity. In the low mesopic conditions, the patients were instructed not to talk, to remain as still as possible, and to breathe regularly without taking deep breaths. After 15 min of the acclimation period (pre-ISBPB), the pupil diameter was measured in the left eye and then in the right eye. Subsequently, the systolic, diastolic, and mean arterial blood pressures were measured. The measurements were followed by administration of the ISBPB with the lights on. The patients remained still in the supine position with the lights off for 30 min after the ISBPB. The pupil size and arterial blood pressure were measured (post-ISBPB), and then the lights were turned on. The patients were placed in the seated position with the back elevated to 70°–80°; the hips and knees flexed to 30° and 120°, respectively; and the knees rested on a pillow. Following evaluation of the sensory and motor blockade, the patients remained still in the seated position with the lights off for 15 min. The study session ended after the third measurement of the pupil diameter and the blood pressure were taken (post-sitting). The study timeline is illustrated in Fig. 1. All the study cases began and finished between 9:00 am and 12:00 pm. The anesthesiologist who performed the ISBPB was not involved in (and was blinded to) the data collection and analysis. One of the authors extracted and analyzed the PPG waveforms for the last 5 min before each of the first two measurements of the pupil diameter (pre-ISBPB and post-ISBPB) and analyzed the ECG waveforms for the last 5 min before each of the three measurements (pre-ISBPB, post-ISBPB, and post-sitting). Another author measured the pupil diameter, blood pressure, and degree of sensory and motor blockade. Both authors were blinded to each other's data.

At the end of the experiment, the patient was prepared for surgery, and the surgery proceeded with the patient seated. Intraoperatively, ECG and pulse oximetry were monitored continuously. The patient's arterial blood pressure was monitored using a noninvasive blood pressure cuff at 5-min intervals. However, the blood pressure could be measured at any time within the 5-min interval at the discretion of the attending anesthesiologist, who was not involved in the study.

For the placement of ISBPB, a 5- to 13-MHz linear phased array transducer (UST-5413, Hitachi Aloka Medical, Ltd., Japan) equipped in an ultrasound machine (Prosound™ α6, Hitachi Alo-

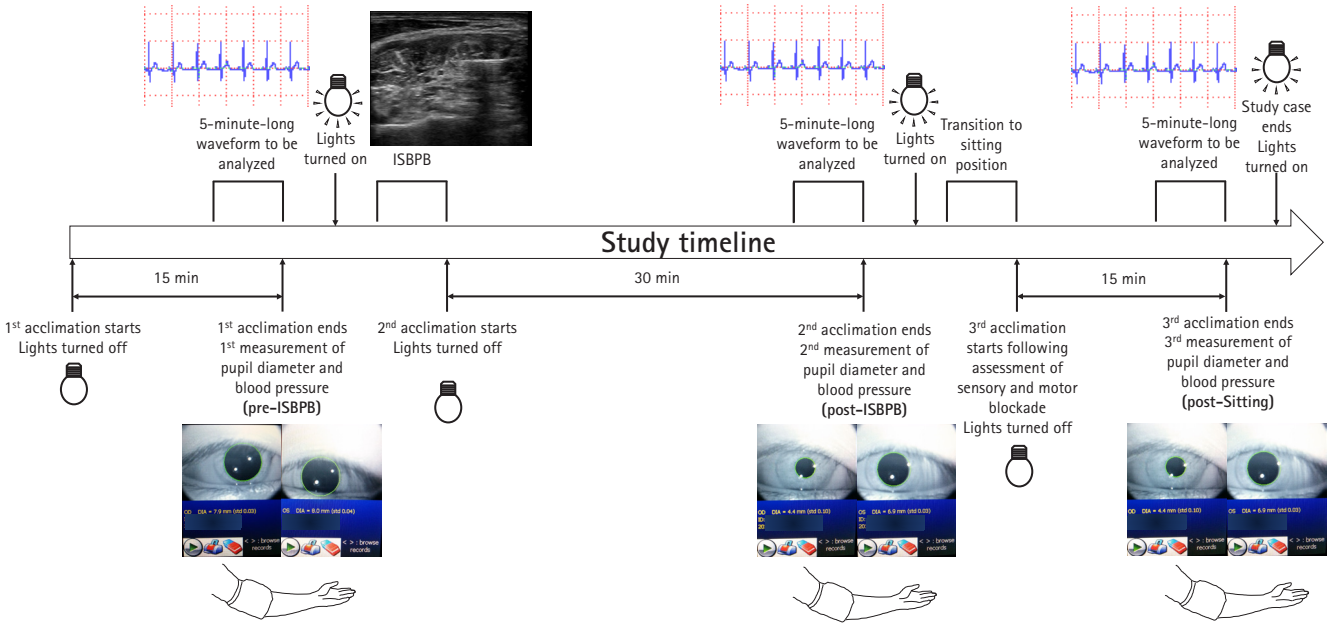

Fig. 1. Experimental design of the study. The study parameters were measured at three time points. ISBPB: interscalene brachial plexus block.

https://doi.org/10.4097/kja.22324

ka Medical, Ltd., Japan) was used to visualize the 5th, 6th, and 7th cervical nerve roots (C5, C6, and C7 nerve roots) [2]. A 50-mm, 22-gauge block needle (SonoPlex STIM, Pajunk® GmbH, Germany) was introduced lateral to the transducer using an in-plane technique and was advanced in a lateromedial direction. Each nerve root and the supraclavicular nerve located between the middle scalene muscle and the posterior border of the sternocleidomastoid muscle [24] were blocked with 25–30 ml of 0.75% ropivacaine.

Following the adaptation to low mesopic conditions [25], the patients were instructed to keep their head and eyes facing forward and their eyes wide open without blinking during the targeting and measurements. The eyecup of an automated monocular infrared pupillometer (VIP™-200 pupillometer, NeurOptics Inc., USA) was placed around the eye being tested and parallel to the axis of vision. The tilt of the instrument was minimized to ensure the best alignment (right angle) between the instrument and the axis of vision. The pupil diameter was measured at 30 Hz for 2 s. Its average and standard deviation were calculated from the 60 measurement data (Supplementary Fig. 1) [1]. If the standard deviation was more than 0.1 mm, the measured value was discarded, and a new measurement was performed. The pupil diameter contralateral to the ISBPB was measured first, and then the ipsilateral diameter was measured.

Between the beginning and end of vital sign monitoring, the ECG and PPG waveforms were continuously recorded at a sampling rate of 300 Hz using S5 collect software (GE Healthcare Finland Oy, Finland) installed in a laptop computer connected to a patient monitor via a UPI-PI Serial Cable (GE Healthcare Finland Oy, Finland). The pulse oximeter sensor was placed on the index finger ipsilateral to the ISBPB before the patients had transitioned from the supine to seated position; afterward, the sensor was placed on the contralateral index finger.

Five-minute-long ECG waveforms for each study time point were loaded onto the WinDaq Waveform Browser (DATAQ Instruments, USA). The R peaks of the ECG signal were automatically detected using Advanced CODAS analysis software (DATAQ Instruments). Undetected or erroneously detected peaks were identified by manual inspection and then manually replaced with new correct peaks or discarded.

The beat-to-beat RR intervals were calculated using Advanced CODAS analysis software. The RR intervals from ectopic beats were defined as those 20% shorter or longer than the previous interval. They were replaced with adjacent normal RR intervals. ECG waveform segments with more than three ectopic beats were excluded from the final analysis. In a tachogram, the abscissa and ordinate represent the time in seconds and RR interval in milliseconds, respectively. Each data point was linearly interpolated, and then new discrete-time equidistant data were generated by resampling at 4 Hz from the interpolated line. By creating a residual plot from the simple linear regression model built with time (independent variable) and corresponding RR interval (dependent variable) resampled at 4 Hz, the tachogram was detrended. The 300-second-long detrended data were split into five segments of 100 s in length with two adjacent segments overlapping by 50% (50 s). Each segment was Hamming windowed [26] and submitted to fast Fourier transform to generate five periodograms. The values of the spectral power corresponding to each frequency from the five periodograms were averaged (Welch method of power spectral density estimation) [27]. The frequency resolution was 0.01 Hz, and the highest frequency of the power spectrum was 2 Hz (Nyquist frequency).

The areas from 0.04 to 0.15 Hz, from 0.15 to 0.4 Hz, and from 0 to 0.4 Hz were integrated to obtain the LF, high-frequency power (HF), and total power of HRV, which represent the combined sympathetic and parasympathetic modulation of the heart rate via baroreceptor reflexes, parasympathetic modulation of heart rate in response to spontaneous respiration, and the overall activity of the autonomic nervous system [28]. Because LF is mainly modulated by SNA [16,17], the LF to HF ratio (LF/HF) represents the sympathovagal balance [28]. Its increase indicates a shift in the sympathovagal balance toward sympathetic predominance, and vice versa. The power spectral density was calculated using the advanced DSP module of DADiSP software version 6.7 (DSP Development Corp., USA). The LF, HF, and total power were natural-log-transformed due to their skewed distribution. Descriptions of the spectrogram, time domain and nonlinear HRV parameters, and sample and approximate entropy are provided in the Supplementary Material 1.

As with the analysis of ECG waveforms, the systolic peaks of the PPG signal were detected using Advanced CODAS analysis software (DATAQ instrument) in the 5-minute-long PPG waveforms for each study time point, which were loaded onto the WinDaq Waveform Browser (DATAQ Instruments). The missing or spurious peaks detected under visual inspection were replaced with new ones or deleted, respectively.

Pulse wave transit time was defined as the time interval between an R peak of the ECG signal and the foot of the PPG wave corresponding to the R peak (the maximum of the second derivative of the PPG wave) [29]. Erroneously detected or undetected maximum peaks of the second derivative were manually deleted or added, respectively. The surgical pleth index (SPI) displayed on the patient monitor was also recorded [30].

A hypotensive bradycardic event (HBE) was determined to oc-

cur 1) if the heart rate decreased by more than 30 beats/min from the pre-ISBPB rate within a 5-min interval or decreased to less than 50 beats/min at any time and/or 2) if the systolic blood pressure decreased by more than 30 mmHg from the pre-ISBPB blood pressure within the 5-min interval or decreased to less than 90 mmHg at any time. However, the presence of signs and symptoms of an HBE (lightheadedness, nausea, vomiting, and cold sweats) were not mandatory for its diagnosis [31]. HBEs were managed with 5–10 mg of ephedrine, the administration of which could be repeated up to three times.

Because the purpose of this study was to assess the usefulness of pupillometry to predict the changes in CSNA following ISBPB, the primary endpoint was the change in pupil diameter from the baseline (pre-ISBPB) to the sitting position (post-sitting), which were adjusted for the baseline difference between the bilateral eyes ([right pupil diameter for post-sitting – left pupil diameter for post-sitting] – [right pupil diameter for pre-ISBPB – left pupil diameter for pre-ISBPB]). The secondary outcome variables were the changes in CSNA from pre-ISBPB to post-sitting (natural-log-transformed LF [lnLF] for post-sitting – lnLF for pre-ISBPB); the right and left pupil diameters; the HRV parameters from the frequency domain, the time domain, and nonlinear analyses; the arterial blood pressure at the three time points; the PPG parameters at the first two time points; the incidence of HBE; and the incidence of Horner's syndrome, which was diagnosed if the adjusted pupil diameter was less than –0.5 mm [32].

Sample size calculation

According to the results of the pilot study using 10 patients, the standard deviation of the changes in pupil diameter adjusted for the baseline differences was 0.4 mm. The regression coefficient and coefficient of determination (R^2) of the linear regression model between the changes in pupil diameter (independent variable) and the changes in lnLF (dependent variable) were 0.5 and 0.21, respectively. A sample size of 42 was required to achieve 90% statistical power at a two-sided significance level of 0.05 for the detection of a change in the regression coefficient from 0 under the null hypothesis to 0.5 under the alternative hypothesis when the coefficient of determination and standard deviation of the independent variable were 0.21 and 0.4 mm, respectively. Considering a drop-out rate of 10%, a total of 48 patients were required in this study. The sample size was calculated using PASS 15 Power Analysis and Sample Size Software (2017) (NCSS, LLC, USA, ncss.com/software/pass).

Statistical analysis

The normality assumption was tested using the Shapiro–Wilk test. Normally and nonnormally distributed data are presented as the mean ± SD and median (Q1, Q3), respectively. Categorical data are presented as the number of patients (percentage). A simple linear regression analysis was performed to investigate the linear relationship between the changes in pupil diameter and the changes in lnLF from baseline to when the patient was in the sitting position. We used a linear mixed-effects model to assess the fixed effects of the side of an eye, three time points, and the interaction between them on the pupil diameter, taking into account the random effects of each subject. The longitudinal changes in the difference in the pupil diameters between bilateral eyes, the HRV parameters, and the arterial blood pressure during the three time points were analyzed using a repeated-measures analysis of variance (for normally distributed data) or Friedman's test (for nonnormally distributed data), with paired t test or Dunn's test used for the post hoc pairwise multiple comparisons, respectively. To compensate for an α error inflation resulting from multiple pairwise comparisons, the probability values were adjusted using the Bonferroni correction. The changes in the PPG parameters during the first two time points were assessed by a paired t test. A two-sided probability value < 0.05 was considered statistically significant. All statistical analyses were performed using IBM SPSS Statistics for Windows (Version 20.0.0, IBM Corp., USA).

Results

Out of 48 recruited patients, six patients were excluded from the analysis due to the development of arrhythmia despite a normal preoperative ECG (n = 1); the presence of severe preoperative ptosis in both eyes, which precluded appropriate measurement of the pupil diameter (n = 1); intolerance to the nearly upright seated position (n = 1); the inability to visualize the C7 nerve root under ultrasound guidance (n = 1); protocol violation (n = 1); and an intolerance to the subjective dyspnea caused by ipsilateral diaphragmatic paralysis, leading to conversion to general anesthesia (n = 1). Table 1 shows the characteristics of the 42 patients whose data were analyzed. Out of the 42 patients, 41 (97.6%) developed Horner's syndrome. The ipsilateral (right) pupil diameter was significantly decreased; the absolute difference in the pupil diameter between ipsilateral (right) and contralateral (left) eyes was significantly increased post-ISBPB and post-sitting compared to pre-ISBPB (Fig. 2). The lnLF, natural-log-transformed HF (lnHF), and natural-log-transformed total power (lnTP) were significantly reduced from baseline (pre-ISBPB) to

https://doi.org/10.4097/kja.22324

Table 1. Patient Characteristics (n = 42)

Variable	Value
Age (yr)	50.0 (30.5, 56.0)
Sex (M/F)	24 (57.1)/18 (42.9)
Height (cm)	165.6 ± 8.4
Weight (kg)	62 (56.8, 69.3)
Surgical procedures	
Rotator cuff repair	26 (61.9)
Labral repair	14 (33.3)
Others	2 (4.8)
Duration of surgery (min)	80.0 ± 29.1

Values are presented as median (Q1, Q3), number of patients (%) or mean ± SD.

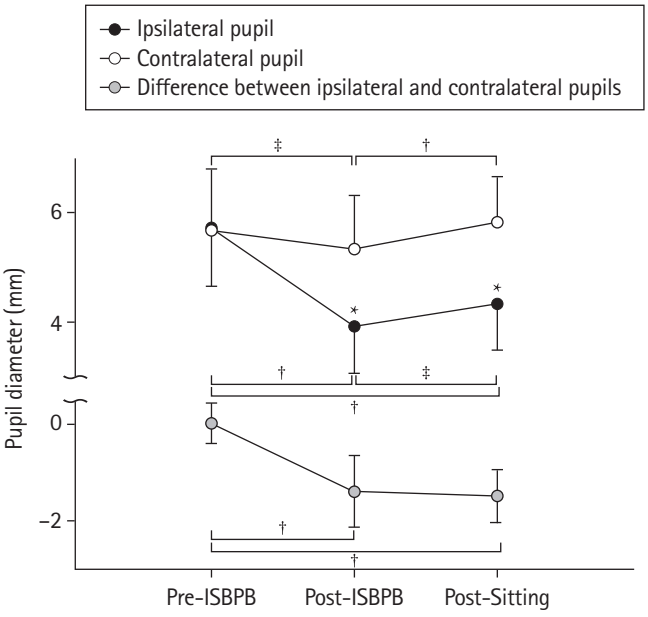

Fig. 2. Longitudinal changes in the bilateral pupil diameters and the difference in the pupil diameters between bilateral eyes. *P < 0.001 compared to the contralateral eye, †P < 0.001, ‡P < 0.01. ISBPB: interscalene brachial plexus block.

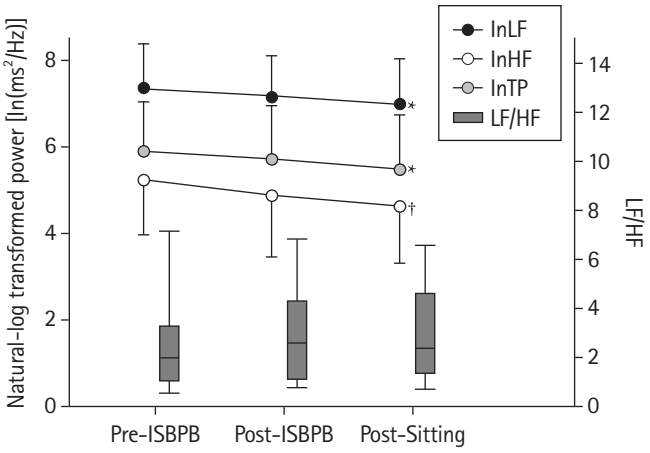

Fig. 3. Longitudinal changes in the spectral parameters of HRV. *P < 0.05 and †P < 0.001 compared to pre-ISBPB. HRV: heart rate variability, ISBPB: interscalene brachial plexus block, LF/HF: low-to-high frequency power ratio, lnHF: natural-log transformed high frequency power, lnLF: natural-log transformed low frequency power, lnTP: natural-log transformed total power.

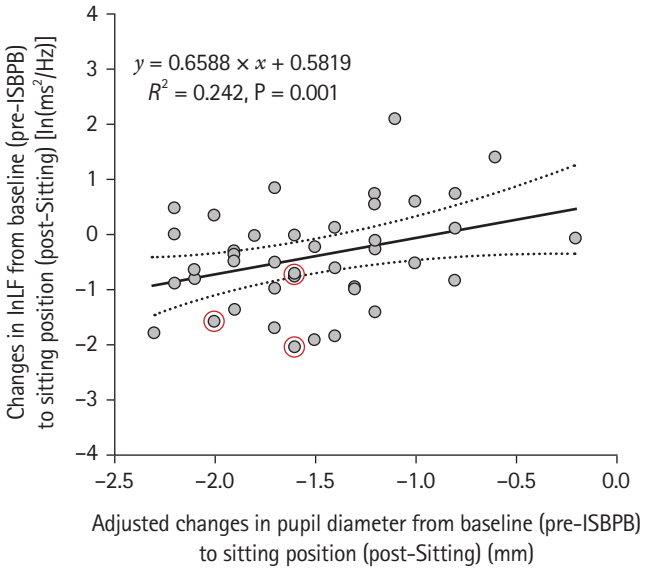

Fig. 4. Simple linear regression analysis between the adjusted changes in pupil diameter and the changes in lnLF from baseline (pre-ISBPB) to sitting position (post-sitting). The three red circles indicate the three patients who developed HBEs. lnLF: natural-log-transformed low-frequency power of HRV, HBEs: hypotensive bradycardic events, HRV: heart rate variability, ISBPB: interscalene brachial plexus block.

the sitting position (post-sitting), while the LF/HF did not change over the three time points (Fig. 3). However, no significant changes in HRV parameters were observed between pre-ISBPB and post-ISBPB or between post-ISBPB and post-sitting. A positive linear relationship was found between the adjusted changes in the pupil diameter and the changes in lnLF from pre-ISBPB to post-sitting (Fig. 4). A one-unit decrease (1 mm) in the change in pupil diameter contributed to a 0.659 ln(ms^2/Hz) decrease in the change in lnLF (95% CI [0.090, 1.228], R^2 = 0.242, P = 0.001).

From pre-ISBPB to post-sitting, there were significant reductions in 1) the proportion of the number of interval differences of successive RR intervals greater than 50 msec in the total number of RR intervals (pNN50); 2) standard deviation of the successive differences of the RR intervals (SDSD); 3) root mean square of the successive differences of the RR intervals (rMSSD); 4) difference between the first and the third quartiles of the successive differ-

ences in the RR intervals (IRRR); 5) median of the absolute values of the successive differences in the RR intervals (MADRR); 6) the baseline width of the triangular interpolation of the NN (RR) interval histogram (TINN); 7) ratio of total number of RR intervals to the number of RR intervals in a 7.8125 msec-long bin with the most RR intervals (HRV index); and 8) standard deviation of the points perpendicular to the line of identity in the Poincaré plot (SD1) (Table 2). The standard deviation of the NN (RR) interval (SDNN), IRRR, TINN, HRV index, and standard deviation along the line of identity in the Poincaré plot (SD2) decreased significantly from pre-ISBPB to post-ISBPB. Although the mean arterial blood pressure and diastolic blood pressure increased significantly from baseline (pre-ISBPB), the heart rate did not change over the three time points. Pulse wave transit time, SPI, and peripheral oxygen saturation were significantly reduced from pre-ISBPB to post-ISBPB, while the PPG amplitude significantly increased (Table 3).

Three patients (7.1%), who included a 46-year-old male, a 58-year-old female, and a 52-year-old female, experienced HBEs 27, 96, and 63 min after the beginning of surgery (72, 146, and 163 min after transitioning to the seated position) and were treated with 10, 10, and 20 mg of ephedrine, respectively. As indicated by the three red circles in Fig. 4, the three patients' absolute differences in lnLF and pupil diameter between pre-ISBPB and post-sitting were greater than their mean differences — 0.413 ln(ms^2/Hz) for lnLF and 1.51 mm for pupil diameter. The spectrogram from one of these patients is presented in Supplementary Fig. 2.

Discussion

According to the results of our study, transitioning to the sitting position following right ISBPB reduced the baseline ipsilateral pupil size, CSNA, and parasympathetic nervous activity but did not change the sympathovagal balance. The extent of the changes in pupil size was positively correlated with that of the changes in SNA before ISBPB and after transition to the seated position following ISBPB.

The ISBPB-induced reduction in pupil size (miosis is one of the clinical signs of Horner's syndrome) is attributed to the blockade of the stellate ganglion, to which local anesthetic placed around the brachial plexus spreads from the interscalene groove along the prevertebral fascia [3]. Because the stellate ganglion is a part of the

Table 2. Changes in the Blood Pressure and Time Domain and Nonlinear HRV Parameters

Variable	Pre-ISBPB	Post-ISBPB	Post-sitting	P value for within-subject effect
Heart rate (bpm)	65.7 (58.5, 72.0)	65.5 (61.2, 71.2)	64.5 (61.9, 72.5)	0.046
SDNN (msec)	39.4 (31.1, 52.1)	37.3 (27.2, 50.1)*	38.8 (25.0, 55.9)	0.042
pNN50 (%)	3.6 (0.8, 15.6)	2.3 (0.3, 19.7)	2.4 (0.0, 8.6)*	0.019
SDSD (msec)	25.0 (17.7, 37.3)	20.3 (13.7, 39.7)	20.2 (12.5, 32.4)†	0.002
rMSSD (msec)	25.0 (17.7, 37.2)	20.3 (13.7, 39.6)	20.2 (12.5, 32.4)†	0.002
IRRR (msec)	47.5 (40.0, 68.8)	43.3 (33.3, 62.7)†	45.0 (30.0, 65.0)†	0.002
MADRR (msec)	16.7 (11.3, 23.3)	13.3 (10.0, 26.7)	13.3 (6.7, 20.4)†	0.001
TINN (msec)	137.6 (116.7, 190.5)	119.0 (93.1, 166.6)*	118.3 (89.4, 162.9)†	0.003
HRV index	8.8 (7.5, 12.2)	7.6 (6.0, 10.7)*	7.6 (5.7, 10.4)†	0.003
SD1	17.7 (12.5, 26.4)	14.4 (9.7, 28.1)	14.3 (8.9, 22.9)†	0.002
SD2	52.1 (41.1, 69.8)	47.8 (37.1, 66.0)*	52.7 (34.4, 76.4)	0.042
SD1/SD2	0.31 (0.25, 0.43)	0.31 (0.25, 0.46)	0.32 (0.22, 0.40)	0.234
Sample entropy	1.42 ± 0.32	1.42 ± 0.34	1.38 ± 0.38	0.721
Approximate entropy	1.04 ± 0.10	1.04 ± 0.11	1.02 ± 0.12	0.463
Systolic blood pressure (mmHg)	121.0 (110.8, 136.3)	125.5 (114.8, 142.3)	126.0 (114.0, 142.5)	0.050
Diastolic blood pressure (mmHg)	74.5 (66.8, 85.8)	76.5 (69.0, 87.3)*	78.0 (70.8, 85.3)†	0.001
Mean arterial blood pressure (mmHg)	92.0 (85.0, 103.8)	95.0 (87.8, 109.3)†	97.5 (88.0, 108.0)*	< 0.001

Values are presented as median (Q1, Q3) or mean ± SD. *P < 0.05 and †P < 0.01 compared to pre-ISBPB. ISBPB: interscalene brachial plexus block, SDNN: standard deviation of the NN (RR) interval, pNN50: the proportion of the number of interval differences of the successive RR intervals greater than 50 msec in the total number of RR intervals, SDSD: standard deviation of the successive differences of the RR intervals, rMSSD: root mean square of the successive differences of the RR intervals, IRRR: difference between the first and the third quartiles of the successive differences in the RR intervals, MADRR: median of the absolute values of the successive differences in the RR intervals, TINN: the baseline width of the triangular interpolation of NN (RR) interval histogram, HRV: heart rate variability, HRV index: the ratio of total number of RR intervals to the number of RR intervals in a 7.8125 msec-long bin with the most RR intervals, SD1: standard deviation of the points perpendicular to the line of identity in the Poincaré plot, SD2: standard deviation along the line of identity in the Poincaré plot.

https://doi.org/10.4097/kja.22324

Table 3. Pulse Plethysmography Data

Variable	Pre-ISBPB	Post-ISBPB	Mean difference (95% CI)	P value
Pulse wave transit time (msec)	152.7 ± 21.6	131.3 ± 24.4	−21.4 (−24.6, −18.1)	< 0.001
Amplitude (arbitrary unit)	1.27 ± 0.70	5.08 ± 1.86	3.81 (3.23, 4.38)	< 0.001
Infrared amplitude (%)	5.5 ± 3.0	9.1 ± 3.5	3.5 (2.5, 4.6)	< 0.001
SPI	39.6 ± 14.3	31.4 ± 8.6	−8.2 (−13.2, −3.1)	0.002
Peripheral oxygen saturation	96.1 ± 1.5	94.6 ± 1.6	−1.4 (−1.8, −1.1)	< 0.001

Values are presented as mean ± SD. ISBPB: interscalene brachial plexus block, SPI: surgical pleth index.

second-order (preganglionic) neuron of the oculosympathetic pathway, its blockade blocks the terminal branches (the long ciliary nerves) of the third-order neuron at the anterior segment of the ipsilateral eye. As a result, the iris dilator muscle is relaxed by the unopposed parasympathetic action on the iris sphincter muscle, consequently leading to miosis of the pupil (anisocoria) [33].

The stellate ganglion also gives off the postganglionic fibers that travel to the heart via the cardiac sympathetic pathways [4]. The inferior cervical and 1st thoracic (T1) ganglia from the stellate ganglion form synapses with the inferior cervical and T1 cardiac nerves, respectively. The two sympathetic postganglionic fibers form the cardiac plexuses with other sympathetic postganglionic fibers from the superior and middle cervical ganglia and the 2nd to 5th thoracic paravertebral ganglia, as well as parasympathetic preganglionic fibers (branches of the vagal and recurrent laryngeal nerves) [4]. In particular, sympathetic neurons project from the craniomedial aspect of the right stellate ganglion and travel to the sinoatrial node, which regulates the heart rate [34]. Because periodic impulse formations by the sinoatrial node contribute to the HRV derived from RR intervals (heart rate) [35,36], a right SGB causes specific changes in the HRV parameters.

In the current study, the incidence of Horner's syndrome was 97.6%, and lnLF, lnHF, and lnTP were decreased with no change in LF/HF after transitioning to the sitting position following a right ISBPB, which was similar to the results in a previous study where the incidence of Horner's syndrome was not reported [31]. However, when the patients were in the supine position 30 min after the placement of the right ISBPB (prior to the sitting position), the decreases in the spectral power of HRV were not statistically significant. In another previous study, the incidence of Horner's syndrome was 35.7%, and that study reported significant decreases in lnLF and lnHF in patients in the supine position [37]. Regrettably, the two abovementioned studies [31,37] did not use objective tools to determine the development of Horner's syndrome. Hence, the incidence might be underestimated, so the effects of ISBPB-induced SGB on the HRV parameters are unclear. In contrast, we quantitatively measured the pupil diameter using pupillometry to determine if the patient developed Horner's syndrome and found that most patients developed Horner's syndrome. Therefore, we could measure the changes in autonomic nervous activity according to the various degrees of Horner's syndrome.

lnLF, lnHF, and lnTP were reduced 30 min after a direct block of the right stellate ganglion using 8 ml of 1% mepivacaine in supine patients [38]. In contrast, our study showed no significant changes in those spectral domain HRV parameters, with some decreases in the time domain HRV parameters, which represent both SNA and parasympathetic nervous activity, between 25 and 30 min after ISBPB in the supine position. We assume that the indeterminate amount of a local anesthetic with a slow onset (ropivacaine) leaking outside the interscalene groove to the stellate ganglion and to the adjacent vagal nerve [39] produced a combined sympathetic and parasympathetic blockade, albeit incompletely.

Head-up tilt or the change from the supine to the sitting position after a right SGB caused no significant changes in the HRV parameters, unlike the normal physiologic response of autonomic nervous activity to positional changes (a reduction in HF and an increase in LF/HF) [9,10]. In our study, a change from the supine to the sitting position even reduced both the lnLF and lnHF from baseline without changing the LF/HF, possibly indicating that the incomplete sympathetic and parasympathetic blockade (30 min after ISBPB placement) became more intense more than 40 min after ISBPB placement (far past the onset of ropivacaine).

Because the reduction in CSNA by ISBPB-induced SGB has been assumed to be associated with the development of HBEs in the sitting position [31,40,41], an immediate measurement of CSNA is of utmost importance for patient safety. However, the conventional methods for the measurement of SNA require expensive equipment and technical support and therefore are not useful in intraoperative settings [13]. As one of the intraoperative standard monitoring parameters, ECG can be used for HRV analysis to noninvasively measure cardiac autonomic nervous activity. However, HRV analysis cannot provide instantaneous information about CSNA because at least 4 min are required to obtain LF values [18]. In addition, at least 10 min of acclimation time stabilizing the patients' autonomic nervous activity is required to ob-

tain reliable HRV parameters [31]. Furthermore, ECG waveforms are prone to artifacts that are caused by patient movement [42] or the use of electrocauterization to prevent bleeding [43]. The calculation of HRV variables with preprocessing of ECG waveforms is also time consuming. In contrast, the measurement of pupil diameter using a pupillometer is more feasible because it requires only 2 s (in this study) and is resistant to artifacts [19]. In addition, because pupil size reaches a plateau within seconds in a dark condition, its measurements require a few seconds of adaptation [44]. Given that SGB acts on both the oculosympathetic and cardiac sympathetic pathways, we expected that the changes in the pupil diameter reflected those in CSNA and found a significant linear correlation between them. Therefore, as an alternative to LF, pupillometry can be useful to assess the changes in CSNA after assuming the sitting position under the influence of an ISBPB-induced SGB.

An increase in the PPG amplitude is consistent with an increase in the blood flow of the ipsilateral upper limb after ISBPB [45,46]. However, because SGB alone can also increase the blood flow of the ipsilateral upper limb [47], we could not differentiate the effects of ISBPB and SGB on blood flow. In addition, the pulse wave transit time was reduced after ISBPB, which is contrary to the results of previous studies that showed that it increased after axillary brachial plexus block [48] and SGB [49]. Therefore, further studies are warranted to investigate the difference in the results between the previous study and ours.

Some limitations should be considered in this study. First, the pupil sizes were not measured while recording the ECG waveforms because the placement of a pupillometer on the eye would affect cardiac autonomic nervous activity by making the patients nervous, leading to ineffective assessments of the effects of ISBPB on cardiac autonomic nervous activity. Second, HRV analysis cannot assess the authentic effects of ISBPB-induced SGB on cardiac autonomic nervous activity because, in addition to the stellate ganglion, the superior and middle cervical ganglia and the 2nd to 5th thoracic paravertebral ganglia also contribute to CSNA. Therefore, the effects of ganglia other than the stellate ganglion on CSNA might have generated some significant errors that reduced the predictability of the regression model derived from the pupil size and lnLF changes. In this regard, the use of pupil size is limited in the assessment of how CSNA is affected by ISBPB-induced SGB. Nonetheless, we tried to exclude the effects of the above-mentioned ganglia by giving patients sufficient acclimation time to stabilize their autonomic nervous activity. However, further studies are warranted to exclude the effects of ganglia other than the stellate ganglion and inconsistencies in the timing of measurement between pupil size and HRV. Third, due to the low incidence of HBEs in this study (3 out of 42 patients), the clinical usefulness of pupillometry to detect the development of HBEs could not be assessed. However, all three patients who developed HBEs had relatively large reductions in both the pupil size and lnLF. We hope that these three cases inspire further studies to investigate the usefulness of pupillometry to detect the development of HBEs. Last, a Bland–Altman agreement analysis could not be used to determine the agreement between the two methods (HRV and pupillometry) that measured the CSNA because they have different units — ln(ms^2/Hz) versus mm. Therefore, we alternatively performed a simple linear regression to compare the two methods [50].

Our results showed that the changes in pupil size were linearly proportional to the changes in CSNA before ISBPB and after sitting following ISBPB. In conclusion, as an alternative to HRV, pupillometry can be used to measure the changes in CSNA after patients are placed in a sitting position after ISBPB.

Funding

This work was supported by the Research Institute of Medical Science, Daegu Catholic University, Republic of Korea (No. 201802).

Conflicts of Interest

No potential conflict of interest relevant to this article was reported.

Data Availability

The datasets generated during and/or analyzed during the current study are available from the corresponding author on reasonable request.

Author Contributions

Eugene Kim (Conceptualization; Data curation; Formal analysis; Investigation; Methodology; Writing – original draft; Writing – review & editing)
Jung A Lim (Conceptualization; Data curation; Formal analysis; Investigation; Methodology; Visualization; Writing – original draft; Writing – review & editing)
Chang Hyuk Choi (Data curation; Formal analysis; Investigation; Methodology; Validation; Visualization; Writing – review & editing)
So Young Lee (Data curation; Formal analysis; Investigation;

https://doi.org/10.4097/kja.22324

Methodology; Software; Validation; Visualization; Writing – review & editing)
Seongmi Kwak (Formal analysis; Investigation; Methodology; Software; Validation; Visualization; Writing – review & editing)
Jonghae Kim (Conceptualization; Data curation; Formal analysis; Funding acquisition; Investigation; Methodology; Project administration; Software; Supervision; Validation; Visualization; Writing – original draft; Writing – review & editing)

Supplementary Materials

Supplementary Marterial 1. Generation of heart rate variability spectrogram and calculation of time domain/non-linear parameters of heart rate variability and sample/approximate entropy.
Supplementary Fig. 1. Measurements of the bilateral pupil diameters using a portable pupillometer. (A) Before interscalene brachial plexus block. The pupils are isocoric. (B) Thirty minutes after interscalene brachial plexus block, miosis of the right eye (OD) was observed. The numbers before the unit (mm) represent the mean pupil diameters measured at 30 Hz for 2 s. OD: oculus dextrus, OS: oculus sinister, DIA: diameter, std: standard deviation.
Supplementary Fig. 2. The spectrogram and trends in the low-frequency power, high-frequency power, low-frequency to high-frequency power ratio, heart rate (computed from the instantaneous RR intervals), and blood pressure throughout the surgery of a 52-year-old female patient with an adjusted change in PD and change in lnLF of –1.6 mm and –2.04 ln(ms^2/Hz), respectively. This patient developed a hypotensive bradycardic event 63 min after the beginning of the surgery (163 min after the sitting position). Significant surges of low-frequency power and a low-frequency to high-frequency power ratio were accompanied by a hypotensive bradycardic event. ISBPB: interscalene brachial plexus block, PD: pupil diameter, BP: blood pressure. lnLF: natural-log-transformed low-frequency power of heart rate variability.

ORCID

Eugene Kim, https://orcid.org/0000-0002-1926-4191
Jung A Lim, https://orcid.org/0000-0002-7427-5483
Chang Hyuk Choi, https://orcid.org/0000-0003-1201-9828
So Young Lee, https://orcid.org/0000-0001-8307-9698
Seongmi Kwak, https://orcid.org/0000-0003-4543-8666
Jonghae Kim, https://orcid.org/0000-0003-1222-0054

References

1. Kim E, Choi CH, Kim JH. Effects of C8 nerve root block during interscalene brachial plexus block on anesthesia of the posterior shoulder in patients undergoing arthroscopic shoulder surgery: study protocol for a prospective randomized parallel-group controlled trial. Trials 2019; 20: 533.
2. Ryu T, Kil BT, Kim JH. Comparison between ultrasound-guided supraclavicular and interscalene brachial plexus blocks in patients undergoing arthroscopic shoulder surgery: a prospective, randomized, parallel study. Medicine (Baltimore) 2015; 94: e1726.
3. Basaran B, Yilbas AA, Gultekin Z. Effect of interscalene block on intraocular pressure and ocular perfusion pressure. BMC Anesthesiol 2017; 17: 144.
4. Wink J, van Delft R, Notenboom RG, Wouters PF, DeRuiter MC, Plevier JW, et al. Human adult cardiac autonomic innervation: controversies in anatomical knowledge and relevance for cardiac neuromodulation. Auton Neurosci 2020; 227: 102674.
5. Wittwer ED, Radosevich MA, Ritter M, Cha YM. Stellate ganglion blockade for refractory ventricular arrhythmias: implications of ultrasound-guided technique and review of the evidence. J Cardiothorac Vasc Anesth 2020; 34: 2245-52.
6. Tian Y, Wittwer ED, Kapa S, McLeod CJ, Xiao P, Noseworthy PA, et al. Effective use of percutaneous stellate ganglion blockade in patients with electrical storm. Circ Arrhythm Electrophysiol 2019; 12: e007118.
7. Cha YM, Li X, Yang M, Han J, Wu G, Kapa SC, et al. Stellate ganglion block and cardiac sympathetic denervation in patients with inappropriate sinus tachycardia. J Cardiovasc Electrophysiol 2019; 30: 2920-8.
8. Peruto CM, Ciccotti MG, Cohen SB. Shoulder arthroscopy positioning: lateral decubitus versus beach chair. Arthroscopy 2009; 25: 891-6.
9. Nacitarhan V, Elden H, Kisa M, Kaptanoğglu E, Nacitarhan S. The effects of therapeutic ultrasound on heart rate variability: a placebo controlled trial. Ultrasound Med Biol 2005; 31: 643-8.
10. Koyama S, Sato N, Nagashima K, Aizawa H, Kawamura Y, Hasebe N, et al. Effects of right stellate ganglion block on the autonomic nervous function of the heart: a study using the head-up tilt test. Circ J 2002; 66: 645-8.
11. Kinsella SM, Tuckey JP. Perioperative bradycardia and asystole: relationship to vasovagal syncope and the Bezold-Jarisch reflex. Br J Anaesth 2001; 86: 859-68.
12. Masuda A, Fujiki A. Sinus arrest after right stellate ganglion block. Anesth Analg 1994; 79: 607.
13. Valenza G, Citi L, Saul JP, Barbieri R. Measures of sympathetic and parasympathetic autonomic outflow from heartbeat dynamics. J Appl Physiol (1985) 2018; 125: 19-39.
14. Goldstein DS, Bentho O, Park MY, Sharabi Y. Low-frequency

power of heart rate variability is not a measure of cardiac sympathetic tone but may be a measure of modulation of cardiac autonomic outflows by baroreflexes. Exp Physiol 2011; 96: 1255-61.
15. Boyett M, Wang Y, D'Souza A. CrossTalk opposing view: Heart rate variability as a measure of cardiac autonomic responsiveness is fundamentally flawed. J Physiol 2019; 597: 2599-601.
16. Malik M, Hnatkova K, Huikuri HV, Lombardi F, Schmidt G, Zabel M. CrossTalk proposal: heart rate variability is a valid measure of cardiac autonomic responsiveness. J Physiol 2019; 597: 2595-8.
17. Posada-Quintero HF, Dimitrov T, Moutran A, Park S, Chon KH. Analysis of reproducibility of noninvasive measures of sympathetic autonomic control based on electrodermal activity and heart rate variability. IEEE Access 2019; 7: 22523-31.
18. Bourdillon N, Schmitt L, Yazdani S, Vesin JM, Millet GP. Minimal window duration for accurate HRV recording in athletes. Front Neurosci 2017; 11: 456.
19. Kaltsatou A, Hadjigeorgiou GM, Grigoriou SS, Karatzaferi C, Giannaki CD, Lavdas E, et al. Cardiac autonomic function during intradialytic exercise training. Postgrad Med 2019; 131: 539-45.
20. Kaltsatou A, Kouidi E, Fotiou D, Deligiannis P. The use of pupillometry in the assessment of cardiac autonomic function in elite different type trained athletes. Eur J Appl Physiol 2011; 111: 2079-87.
21. Bär KJ, Schulz S, Koschke M, Harzendorf C, Gayde S, Berg W, et al. Correlations between the autonomic modulation of heart rate, blood pressure and the pupillary light reflex in healthy subjects. J Neurol Sci 2009; 279: 9-13.
22. Okutucu S, Civelekler M, Aparci M, Sabanoglu C, Dikmetas O, Aksoy H, et al. Computerized dynamic pupillometry indices mirrors the heart rate variability parameters. Eur Rev Med Pharmacol Sci 2016; 20: 2099-105.
23. Leftheriotis D, Flevari P, Kossyvakis C, Katsaras D, Batistaki C, Arvaniti C, et al. Acute effects of unilateral temporary stellate ganglion block on human atrial electrophysiological properties and atrial fibrillation inducibility. Heart Rhythm 2016; 13: 2111-7.
24. Maybin J, Townsley P, Bedforth N, Allan A. Ultrasound guided supraclavicular nerve blockade: first technical description and the relevance for shoulder surgery under regional anaesthesia. Anaesthesia 2011; 66: 1053-5.
25. Stockman A, Sharpe LT. Into the twilight zone: the complexities of mesopic vision and luminous efficiency. Ophthalmic Physiol Opt 2006; 26: 225-39.
26. Harris FJ. On the use of windows for harmonic analysis with the discrete fourier transform. Proc IEEE 1978; 66: 51-83.
27. Welch P. The use of fast fourier transform for the estimation of power spectra: a method based on time averaging over short, modified periodograms. IEEE Trans Audio Electroacoust 1967; 15: 70-3.
28. Heart rate variability: standards of measurement, physiological interpretation and clinical use. Task Force of the European Society of Cardiology and the North American Society of Pacing and Electrophysiology. Circulation 1996; 93: 1043-65.
29. van Velzen MH, Loeve AJ, Niehof SP, Mik EG. Increasing accuracy of pulse transit time measurements by automated elimination of distorted photoplethysmography waves. Med Biol Eng Comput 2017; 55: 1989-2000.
30. Huiku M, Uutela K, van Gils M, Korhonen I, Kymäläinen M, Meriläinen P, et al. Assessment of surgical stress during general anaesthesia. Br J Anaesth 2007; 98: 447-55.
31. Kim JH, Song SY, Ryu T, Choi CH, Sung SY, Roh WS. Changes in heart rate variability after sitting following interscalene block. Clin Auton Res 2015; 25: 327-33.
32. Yoo YJ, Yang HK, Hwang JM. Efficacy of digital pupillometry for diagnosis of Horner syndrome. PLoS One 2017; 12: e0178361.
33. Kanagalingam S, Miller NR. Horner syndrome: clinical perspectives. Eye Brain 2015; 7: 35-46.
34. Rajendran PS, Challis RC, Fowlkes CC, Hanna P, Tompkins JD, Jordan MC, et al. Identification of peripheral neural circuits that regulate heart rate using optogenetic and viral vector strategies. Nat Commun 2019; 10: 1944.
35. Rosenberg AA, Weiser-Bitoun I, Billman GE, Yaniv Y. Signatures of the autonomic nervous system and the heart's pacemaker cells in canine electrocardiograms and their applications to humans. Sci Rep 2020; 10: 9971.
36. Schwab JO, Eichner G, Schmitt H, Weber S, Coch M, Waldecker B. The relative contribution of the sinus and AV node to heart rate variability. Heart 2003; 89: 337-8.
37. Simeoforidou M, Vretzakis G, Chantzi E, Bareka M, Tsiaka K, Iatrou C, et al. Effect of interscalene brachial plexus block on heart rate variability. Korean J Anesthesiol 2013; 64: 432-8.
38. Fujiki A, Masuda A, Inoue H. Effects of unilateral stellate ganglion block on the spectral characteristics of heart rate variability. Jpn Circ J 1999; 63: 854-8.
39. Janes RD, Brandys JC, Hopkins DA, Johnstone DE, Murphy DA, Armour JA. Anatomy of human extrinsic cardiac nerves and ganglia. Am J Cardiol 1986; 57: 299-309.
40. Seo KC, Park JS, Roh WS. Factors contributing to episodes of bradycardia hypotension during shoulder arthroscopic surgery in the sitting position after interscalene block. Korean J Anesthesiol 2010; 58: 38-44.
41. Song SY, Roh WS. Hypotensive bradycardic events during shoulder arthroscopic surgery under interscalene brachial plexus

https://doi.org/10.4097/kja.22324

blocks. Korean J Anesthesiol 2012; 62: 209-19.
42. Pérez-Riera AR, Barbosa-Barros R, Daminello-Raimundo R, de Abreu LC. Main artifacts in electrocardiography. Ann Noninvasive Electrocardiol 2018; 23: e12494.
43. Naik BN, Luthra A, Dwivedi A, Jafra A. Artifactual ECG changes induced by electrocautery in a patient with coronary artery disease. J Electrocardiol 2017; 50: 531-3.
44. Zauner J, Plischke H, Strasburger H. Spectral dependency of the human pupillary light reflex. Influences of pre-adaptation and chronotype. PLoS One 2022; 17: e0253030.
45. Dorlas JC, Nijboer JA. Photo-electric plethysmography as a monitoring device in anaesthesia. Application and interpretation. Br J Anaesth 1985; 57: 524-30.
46. Iskandar H, Wakim N, Benard A, Manaud B, Ruel-Raymond J, Cochard G, et al. The effects of interscalene brachial plexus block on humeral arterial blood flow: a Doppler ultrasound study. Anesth Analg 2005; 101: 279-81.
47. Kim MK, Yi MS, Park PG, Kang H, Lee JS, Shin HY. Effect of stellate ganglion block on the regional hemodynamics of the upper extremity: a randomized controlled trial. Anesth Analg 2018; 126: 1705-11.
48. Kortekaas MC, Niehof SP, van Velzen MH, Galvin EM, Huygen FJ, Stolker RJ. Pulse transit time as a quick predictor of a successful axillary brachial plexus block. Acta Anaesthesiol Scand 2012; 56: 1228-33.
49. Kim YU, Cheong Y, Kong YG, Lee J, Kim S, Choi HG, et al. The prolongation of pulse transit time after a stellate ganglion block: an objective indicator of successful block. Pain Res Manag 2015; 20: 305-8.
50. Bland JM, Altman DG. Applying the right statistics: analyses of measurement studies. Ultrasound Obstet Gynecol 2003; 22: 85-93.